NASA/TM—2015-218830

Gear Tooth Wear Detection Algorithm

Irebert R. Delgado
Glenn Research Center, Cleveland, Ohio

July 2015

NASA STI Program . . . in Profile

Since its founding, NASA has been dedicated to the advancement of aeronautics and space science. The NASA Scientific and Technical Information (STI) Program plays a key part in helping NASA maintain this important role.

The NASA STI Program operates under the auspices of the Agency Chief Information Officer. It collects, organizes, provides for archiving, and disseminates NASA's STI. The NASA STI Program provides access to the NASA Technical Report Server—Registered (NTRS Reg) and NASA Technical Report Server—Public (NTRS) thus providing one of the largest collections of aeronautical and space science STI in the world. Results are published in both non-NASA channels and by NASA in the NASA STI Report Series, which includes the following report types:

- TECHNICAL PUBLICATION. Reports of completed research or a major significant phase of research that present the results of NASA programs and include extensive data or theoretical analysis. Includes compilations of significant scientific and technical data and information deemed to be of continuing reference value. NASA counter-part of peer-reviewed formal professional papers, but has less stringent limitations on manuscript length and extent of graphic presentations.

- TECHNICAL MEMORANDUM. Scientific and technical findings that are preliminary or of specialized interest, e.g., "quick-release" reports, working papers, and bibliographies that contain minimal annotation. Does not contain extensive analysis.

- CONTRACTOR REPORT. Scientific and technical findings by NASA-sponsored contractors and grantees.

- CONFERENCE PUBLICATION. Collected papers from scientific and technical conferences, symposia, seminars, or other meetings sponsored or co-sponsored by NASA.

- SPECIAL PUBLICATION. Scientific, technical, or historical information from NASA programs, projects, and missions, often concerned with subjects having substantial public interest.

- TECHNICAL TRANSLATION. English-language translations of foreign scientific and technical material pertinent to NASA's mission.

For more information about the NASA STI program, see the following:

- Access the NASA STI program home page at http://www.sti.nasa.gov

- E-mail your question to help@sti.nasa.gov

- Fax your question to the NASA STI Information Desk at 757-864-6500

- Telephone the NASA STI Information Desk at 757-864-9658

- Write to:
  NASA STI Program
  Mail Stop 148
  NASA Langley Research Center
  Hampton, VA 23681-2199

NASA/TM—2015-218830

Gear Tooth Wear Detection Algorithm

Irebert R. Delgado
Glenn Research Center, Cleveland, Ohio

National Aeronautics and
Space Administration

Glenn Research Center
Cleveland, Ohio 44135

July 2015

This work was sponsored by the Fundamental Aeronautics Program at the NASA Glenn Research Center.

Level of Review: This material has been technically reviewed by technical management.

Available from

NASA STI Program
Mail Stop 148
NASA Langley Research Center
Hampton, VA 23681-2199

National Technical Information Service
5285 Port Royal Road
Springfield, VA 22161
703-605-6000

This report is available in electronic form at http://www.sti.nasa.gov/ and http://ntrs.nasa.gov/

Gear Tooth Wear Detection Algorithm

Irebert R. Delgado
National Aeronautics and Space Administration
Glenn Research Center
Cleveland, Ohio 44135

Abstract

Vibration-based condition indicators continue to be developed for Health Usage Monitoring of rotorcraft gearboxes. Testing performed at NASA Glenn Research Center have shown correlations between specific condition indicators and specific types of gear wear. To speed up the detection and analysis of gear teeth, an image detection program based on the Viola-Jones algorithm was trained to automatically detect spiral bevel gear wear pitting. The detector was tested using a training set of gear wear pictures and a blind set of gear wear pictures. The detector accuracy for the training set was 75 percent while the accuracy for the blind set was 15 percent. Further improvements on the accuracy of the detector are required but preliminary results have shown its ability to automatically detect gear tooth wear. The trained detector would be used to quickly evaluate a set of gear or pinion pictures for pits, spalls, or abrasive wear. The results could then be used to correlate with vibration or oil debris data. In general, the program could be retrained to detect features of interest from pictures of a component taken over a period of time.

Background

To aid the analysis of vibration condition indicator data, used to detect damage during spiral bevel gear failure progression tests, a MATLAB (The Mathworks, Inc., Natick, MA) program is being developed to automate the detection and catalog of gear tooth damage from existing digital photographs. The gears are similar to those used in rotorcraft transmissions. Testing was conducted at NASA Glenn Research Center's Spiral Bevel Gear Test Facility, Figure 1. The U.S. Army's Health Usage Monitoring System (HUMS) uses condition indicators (CIs) derived from vibration data to monitor the health of rotorcraft mechanical components and systems including the nose gearbox. The test program at NASA was conducted partly to improve condition indicator performance in correctly identifying gear wear modes such as pitting, scuffing, or spalling (Ref. 1).

During testing, hundreds of gear tooth wear pictures are taken on a single gear/pinion pair. Manually cataloging each of the hundreds of pictures per ANSI/AGMA standards would be time-consuming. A MATLAB algorithm was developed to improve this process of cataloging observed gear wear. Specifically, MATLAB's Computer Vision software was trained to detect and quantify pits, spalls, and scuffing wear occurring on the gear teeth during testing. Preliminary results are given on the accuracy of detecting and quantifying observed gear wear on tests conducted on the NASA Glenn Spiral Bevel Gear Rig test facility. The program was validated with a subset of spiral bevel gear pictures. Details of the validation are given below.

Identifying and categorizing gear tooth wear data and its progression during inspections and when maintenance is performed is part of a process to ultimately improve condition indicator performance for rotorcraft. Research continues in improving condition indicator performance. Dempsey and others (Ref. 2) provide an overview of HUMS and the current use of vibration-based condition indicators. Lessons learned and challenges associated with HUMS systems for rotorcraft drivetrains are given by Zakrajsek and others (Ref. 3). A paper by Antolick and others (Ref. 4) rates various vibration-based condition indicators on actual rotorcraft gearbox data. Dempsey (Ref. 1) showed how condition indicator performance can vary between flight gear box data and test rig data which used similarly designed spiral bevel gears. Romano and others (Ref. 5) demonstrate a software architecture and methodology that

enhances diagnostics and prognostics for rotorcraft drivetrains relative to condition-based maintenance. He and Bechhoefer (Ref. 6) demonstrate a methodology to set condition indicator thresholds.

Because of the large amounts of data generated in HUMS systems (e.g., vibration, CI, gear wear photos), automation of any tasks associated with the gathering, analysis, and storage of these types of data would be beneficial. Automatic feature detection has been implemented in various fields involving large data sets and a need for accuracy and speed. These fields include face detection (Ref. 7), bridge cables (Ref. 8), concrete crack detection, (Ref. 9) machine tool condition, (Ref. 10) and medicine (Ref. 11). Figure 2 shows a notional framework in analyzing gear tooth wear: (1) Detecting/Cataloging of the gear tooth wear feature, (2) Wear feature capture, (3) Data analysis, and (4) Data storage and recall. Detecting and cataloging gear tooth wear may involve the use of algorithms (e.g., Viola-Jones) to detect a wear feature per a gear wear standard (e.g., ANSI/AGMA 1010). Capturing the wear feature would key on a process that is consistent and accurate. Analysis of the data relative to gear wear feature, focuses on correlating the wear feature to vibration or oil-debris data. This would provide feed-back on CI performance and possibly insight into improving the CI. Finally, the ability to store and recall data could provide a means to quickly compare observed gear wear with historical data. A high level of automation would be in-situ processes relating to these four tasks (e.g., auto detection, auto-feature capture, real-time data analysis, online database accessibility). For example, on-board real-time HUMS data analysis of the helicopter gearbox would be preferred rather than after the helicopter has completed its flight, mission, or test.

Objectives

Figure 2 shows a notional framework for the detection, capture, analysis, and storage of gear tooth wear data with the intent of automating individual processes. This paper specifically addresses gear tooth wear feature detection and capture. Observed gear tooth damage is categorized and defined by ANSI/ AGMA 1010 Standards, Appearance of Gear Teeth: Terminology of Wear and Failure (Ref. 12). The Contact Fatigue class is shown in Figure 3. Gear pitting damage is classified under contact fatigue which is subdivided into three general modes: pitting (macropitting), micropitting, and subcase fatigue. Macropitting is further divided into specific modes or degrees, including initial pitting, progressive pitting, flaking, and spalling. Micropitted gears, Figure 4(a), appear frosted, matted, or gray stained. The magnified surface appears to be covered with fine pits. Initially pitted gears, Figure 4(b), exhibit pits less than 1 mm in diameter and are localized on the tooth surface. Progressive pits, Figure 4(c) are significantly larger than 1 mm in diameter. Pitting of this type may continue at an increased rate until a significant portion of the tooth surface has pits of various shapes and sizes. Spalling, Figure 4(d), is progressive pitting where pits coalesce and form irregular craters that cover a significant area of the tooth surface. The scope of this study was limited to accurately detecting both initial and progressive pitting. No attempt was made, at this time, to distinguish between either types of pitting.

An objective of this work would be to automate the detection, cataloging, and capture of gear wear observed on the gear teeth. Large data sets could be catalogued quickly and accurately. A database of results could be queried by users to determine trends in the test data. Addressing the analysis box in Figure 2, these trends could be correlated with existing vibration and oil debris data. Corresponding gear vibration and condition indicators could be improved by fusing this correlation between observed gear wear, vibration, and oil debris data. Ultimately, the improved gear vibration and condition indicators could be implemented on-board HUMS systems for rotorcraft.

Procedure

Hardware

Spiral bevel gears were tested in NASA Glenn's Spiral Bevel Gear Rig test facility, Figure 1. It is a closed-loop, torque regenerative system at 560 kW (750 hp) (Ref. 13). Two gear/pinion pairs are tested simultaneously. These particular series of tests use a 19 tooth pinion and 41 tooth gear, Figure 1(a). The

gears were made from a consumable electrode vacuum melted (CEVM) AISI 9310 steel. They were then carburized, hardened, and ground to AGMA quality number 12 standards. Gear specifications include (1) Ratio: 2.158 (41 gear teeth/19 pinion teeth), (2) diametral pitch: 6.4, (3) pressure angle: 20°, (4) spiral angle: 25° (Ref. 14). Prior to testing, baseline gear and pinion tooth photographs are taken, Figure 5. A total of 120 gear tooth pictures are taken per photograph session and saved in both Nikon Electronic File (NEF) and JPG formats. For consistency, four pre-set camera locations are used, Figure 6, corresponding to the two gear/pinion pair locations. Pictures were taken with an SLR camera (Nikon D5100), macro-lens (AF-S Micro Nikkor 60 mm f/2.8G ED), and flash unit (Metz Mecablitz SCA 300).

During these set of tests the gear/pinion pairs were run-in at a lower load setting prior to the full load setting. Photographs of the gear teeth were taken before and after the lower load run. Thereafter, tests were continuously run at full load until vibration or oil debris minimum levels were exceeded. Gear and pinion tooth wear are photographed during these stops in testing. Testing then continued until tooth pitting damage exceeded 3 to 4 teeth on either a gear or pinion. These gear wear pictures were then processed by the Viola-Jones feature detection algorithm in an attempt to detect pitting damage on the gear teeth.

Software

The Viola-Jones algorithm is provided in MATLAB's Computer Vision System Toolbox. Motivated originally by the problem of face detection (Ref. 15), the algorithm uses stages of weak learners, or simple classifiers, that quickly window through a region for objects of interest. Positive features are passed onto the next stage for further identification. A cascade classifier which is a series of weak learners organized like a decision tree, Figure 7, was trained using a GUI (Ref. 16) provided by MATLAB. Individual and multiple gear tooth pictures were provided showing examples of gear tooth pitting. The user manually selects the pits in the picture. Pictures of gear teeth without pits were also given to provide negative examples to the classifier. Finally the orientation, contrast, and brightness of the pictures were adjusted to give additional examples to the classifier. Table 1 shows these and additional parameters used to train the classifier. The feature type, Histograms of Orientated Gradients (HOG), is useful in determining overall feature shape. The other selectable features, Haar and Local Binary Patterns (LBP), are used to detect fine scale textures. The HOG feature was chosen for this set of analyses. A total of 44 positive and 88 negative examples were used to train the classifier.

Testing

A control test of eight images was run to verify that the detector could identify pits. The pictures used were the same as those to train the detector. A subset of those pictures are shown in Figure 8. The spall shown in Figure 8(d) was chosen as a 'negative' case or 'not a pit'. A cropped set of pictures showing only the center tooth were also used for the control set. A total of 4 pits were to be identified with two additional pictures showing no pitting and two more pictures showing spalling. Finally, a 'blind' test was performed using a set of pitted gear wear pictures which were not used to train the detector, Figure 9. A total of 11 pits were to be identified. Results of both the control and blind tests are given below.

Results and Discussion

Due to an insufficient number of negative images or 'not a pit' images, the cascade classifier was only able to train 11 of 20 cascade stages taking approximately 38 min. to complete using an HP Z800 workstation.

Figure 10 shows the pit detection results for the Control set of pictures. Identified gear pits are highlighted by the detection program with yellow boxes. A total of 6 of 8 pictures or 75 percent were correctly identified as having a pit or not a pit. The detector also attempted to identify pits on teeth as shown in Figure 10(G) and Figure 10(H). Since by definition spalls are collections of pits that are

coalesced together the detector was not entirely incorrect. Figure 11 shows the pit detection results for the Blind set of pictures. Of the 11 pits to be identified, a total of 20 detections were made with four true positives and zero true negatives. The remaining sixteen detected tooth pits were false positives. Thirteen of the sixteen detected false positives were of a tooth edge type of wear. It should be noted that the detector was not trained for this wear type. Three of the identified false positives were located on the tooth face. Seven pits were not identified by the detector and thus are false negatives. The accuracy (Ref. 17) of the detector is given below in
Equation (1). Given the number of true positives (4), number of true negatives (0), false positives (16), and the number of false negatives (7) the resultant accuracy for the Blind set is 15 percent. If the number of tooth edge detections (13) were not considered, then the accuracy is increased to 29 percent. Clearly the detector requires further training with examples of gear tooth wear that is not considered pitting.

$$\text{accuracy} = \frac{\text{True Positives} + \text{True Negatives}}{\text{True Positives} + \text{True Negative} + \text{False Positives} + \text{False Negatives}} \quad (1)$$

While initial results on the detector are promising, further training is needed to improve its accuracy. This would include a sufficient number of examples on tooth edge wear, spalls, and other types of gear wear such as scuffing, abrasion, and fracture. Additional work using Haar and Local Binary Pattern features should be explored to potentially fine tune the detector. Finally, accurately determining the pit size from pictures would further classify pits as described in ANSI/AGMA 1010. For example, knowing the actual dimensions of the gear tooth land, an estimate can be made of the size of the wear feature. Combined with a qualitative assessment of the image the wear feature can then be categorized per ANSI/AGMA 1010 standards. The trained detector would be used to quickly evaluate a set of gear or pinion pictures for pits, spalls, or abrasive wear. The results could then be used to correlate with vibration or oil debris data. In general, the program could be retrained to detect features of interest from pictures of a component taken over a period of time.

Conclusions

To aid in the speed of detection and classification of gear wear during inspections for rotorcraft gearboxes, an image detection algorithm based on the Viola-Jones framework was trained and tested using gear wear pictures from spiral-bevel gear wear tests conducted at NASA Glenn Research Center. The accuracy of the detector for the training set was 75 percent. The accuracy of the detector for the Blind Set was 15 percent. Further improvements on the accuracy of the detector are required. However, preliminary results indicate that the detector has the ability to automatically detect gear tooth wear. The tool can be used correlate gear wear to vibration and oil-debris data as damage initiated and progressed to improve the overall Health Usage Monitoring System.

References

1. Dempsey, P.J. Investigation of Spiral Bevel Gear Condition Indicator Validation Via AC-29-2C Using Damage Progression Tests. NASA/TM—2014-218384.
2. Dempsey, P.J., et al., Investigation of Current Methods to Identify Helicopter Gear Health. Aerospace Conference, 2007 IEEE.
3. Zakrajsek, J.J., et al., Rotorcraft Health Management Issues and Challenges. NASA/TM—2006-214022.
4. Antolick, L.J., et al., Evaluation of Gear Condition Indicator Performance on Rotorcraft Fleet. AHS 66th Annual Forum and Technology Display: Rising to New Heights in Vertical Lift Technology; 11-13 May 2010; Phoenix, AZ; United States.

5. Romano, P., et al., Integrated Software Platform for Fleet Data Analysis, Enhanced Diagnostics, and Safe Transition to Prognostics for Helicopter Component CBM. Annual Conference of the Prognostics and Health Management Society, 2010.
6. He, D., et al., Development and Validation of Bearing Diagnostic and Prognostic Tools using HUMS Condition Indicators. Aerospace Conference, 2008 IEEE.
7. Taigman, Y., et al., DeepFace: Closing the Gap to Human-Level Performance in Face Verification. Computer Vision and Pattern Recognition (CVPR), 2014 IEEE Conference. 1701-1708.
8. Ho, H., et al., An efficient image-based damage detection for cable surface in cable stayed bridges. NDT&E International 58 (2013) 18-23.
9. Lattanzi, D. et al., Robust Automated Concrete Damage Detection Algorithms for Field Applications. Journal of Computing in Civil Engineering March/April 2014.
10. X.Y. Kou, C.S. Wang, L.Li, "A Detection System of Tool Condition Based on Image Processing Technology," Advanced Materials Research, Vol. 510, pp. 375-379, Apr. 2012.
11. Ros, S., et al., Tendon extracellular matrix damage detection and quantification using automated edge detection analysis. Journal of Biomechanics 46 (2013) 2844-2847.
12. ANSI/AGMA 1010-E95. Appearance of Gear Teeth – Terminology of Wear and Failure.
13. Townsend, Dennis P. and Zakrajsek, James J. Evaluation of a Vibration Diagnostic System for the Detection of Spiral Bevel Gear Pitting Failures. NASA TM 107228.
14. Demsey, Paula. Investigation of Spiral Bevel Gear Condition Indicator Validation via AC–29–2C Using Damage Progression Tests. NASA/TM—2014-218384.
15. Viola, P. and Jones, M. Rapid Object Detection using a Boosted Cascade of Simple Features. Computer Vision and Pattern Recognition 2001.
16. http://www.mathworks.com/matlabcentral/fileexchange/39627-cascade-trainer--specify-ground-truth--train-a-detector
17. Šimundić, Ana-Maria. "Measures of diagnostic accuracy: basic definitions." Med Biol Sci 22.4 (2008): 61-5.
18. http://www.mathworks.com/help/vision/ug/train-a-cascade-object-detector.html

TABLE 1.—CASCADE CLASSIFIER TRAINING PARAMETERS

Parameter	Value
Orientation (relative to original picture)	Normal, 180°
Contrast	Normal, +50%, –50%
Brightness	Normal, +50%, –50%
Per stage false alarm rate	0.5
Per stage true positive rate	0.995
Number of cascade stages	20
Feature type	Histograms of Oriented Gradients (HOG)
Negative samples factor	2
Object training size	auto

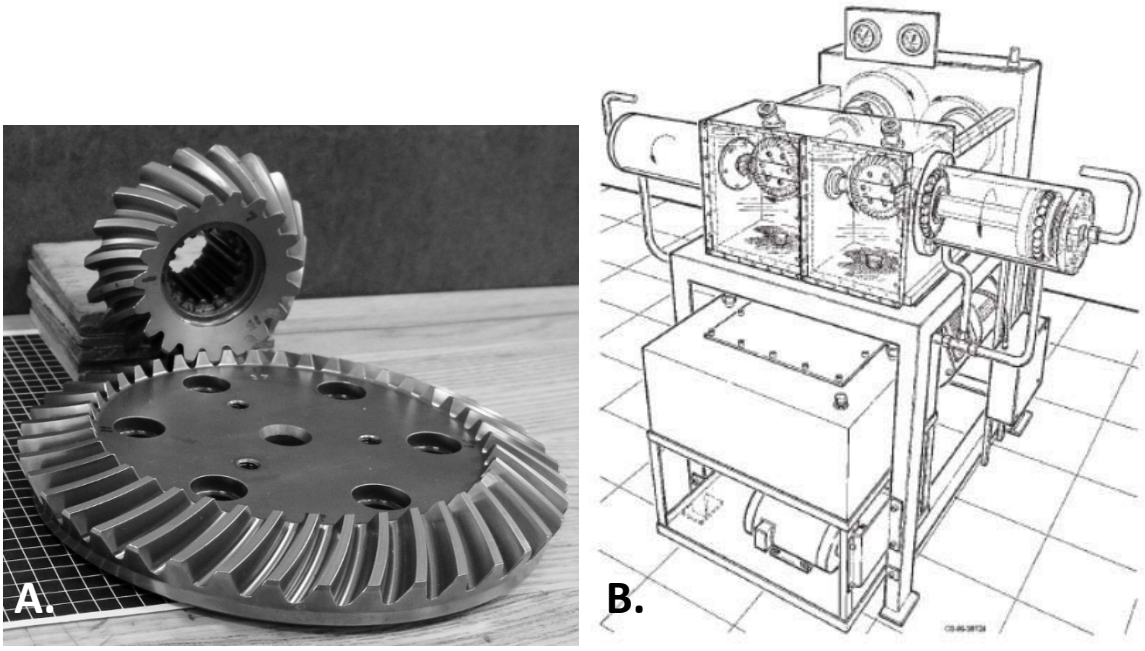

Figure 1.—(A) Example spiral bevel gear pair. (B) NASA spiral bevel gear test rig.

Figure 2.—Notional framework to analyze gear tooth wear.

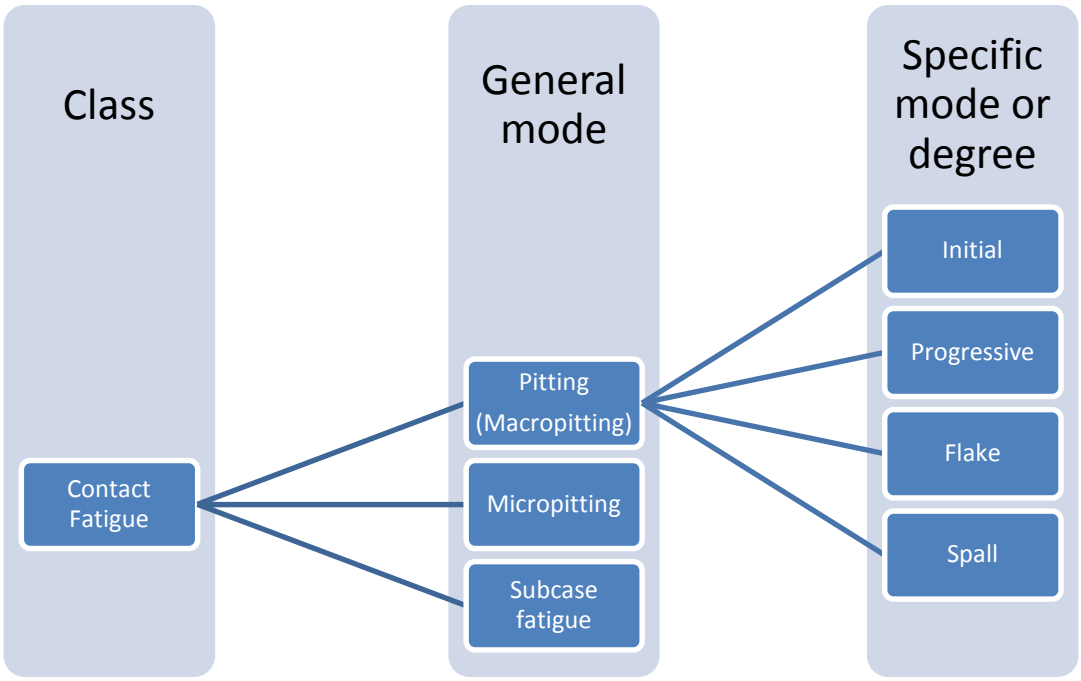

Figure 3.—Gear damage contact fatigue class per ANSI/AGMA 1010 standards (Ref. 12).

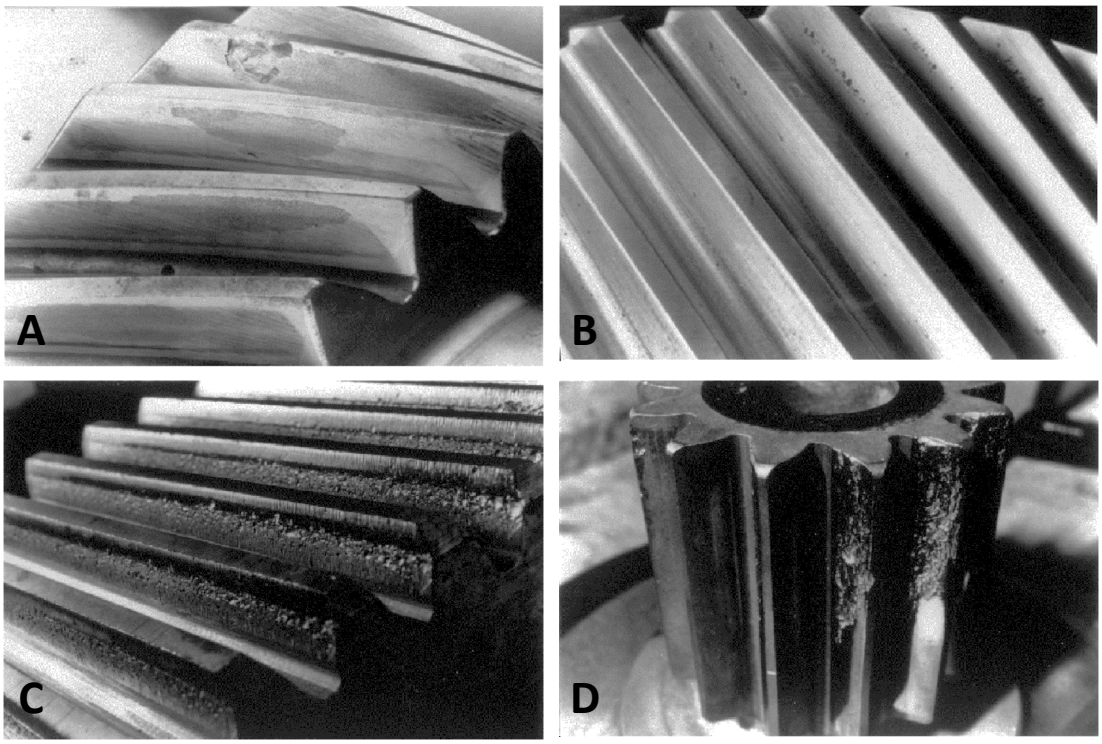

Figure 4.—(A) Micropitting. (B) Initial pitting. (C) Progressive pitting. (D) Spalling. Extracted from ANSI/AGMA 1010-E95, Appearance of Gear Teeth Terminology of Wear and Failure, with the permission of the publisher, the American Gear Manufacturers Association, 1500 King Street, Suite 201, Alexandria, Virginia 22314.

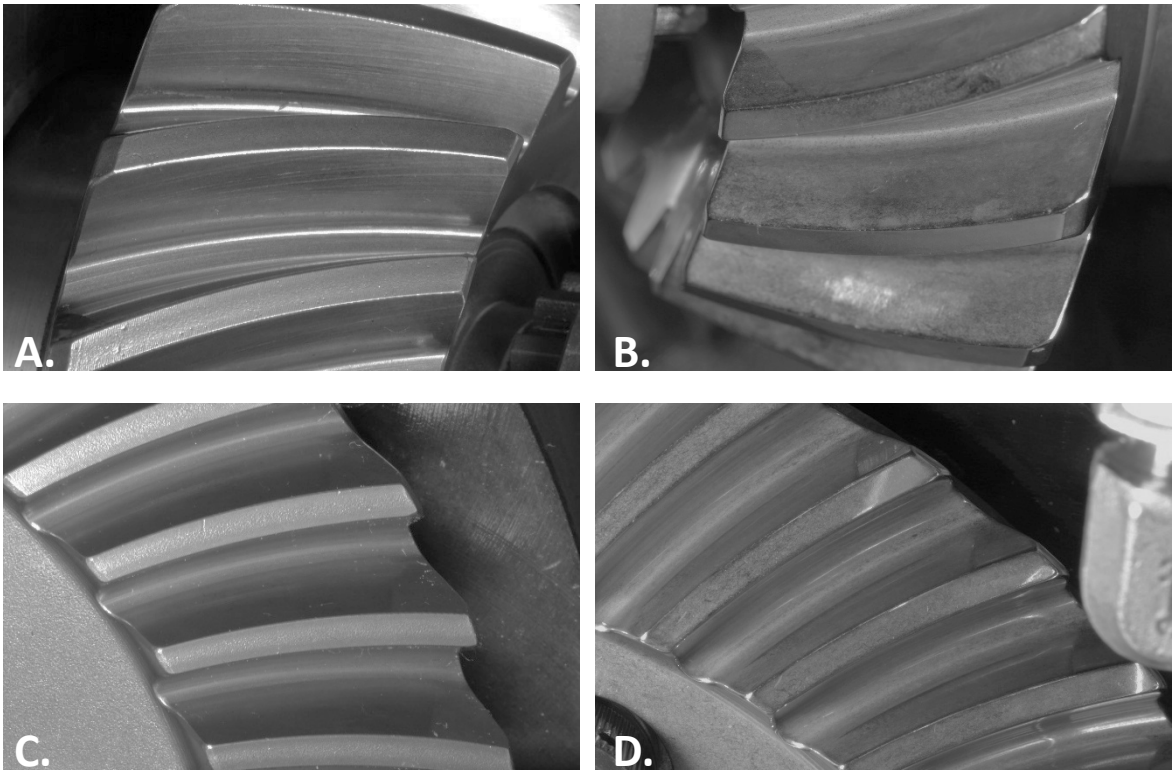

Figure 5.—Baseline gear tooth photographs. (A) Left-hand pinion. (B) Right-hand pinion. (C) Left-hand gear. (D) Right-hand gear.

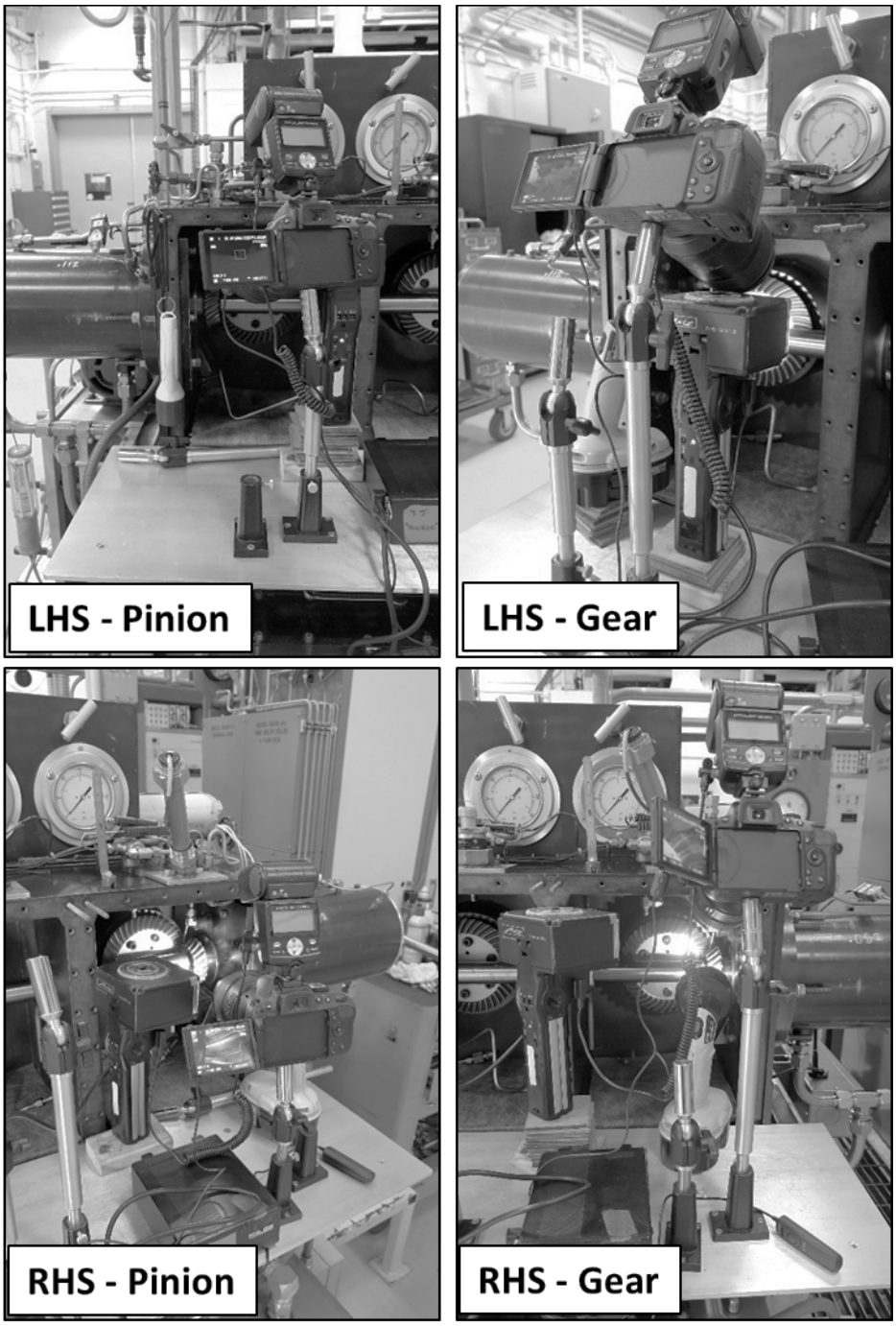

Figure 6.—Pre-set camera positions for gear tooth photos.

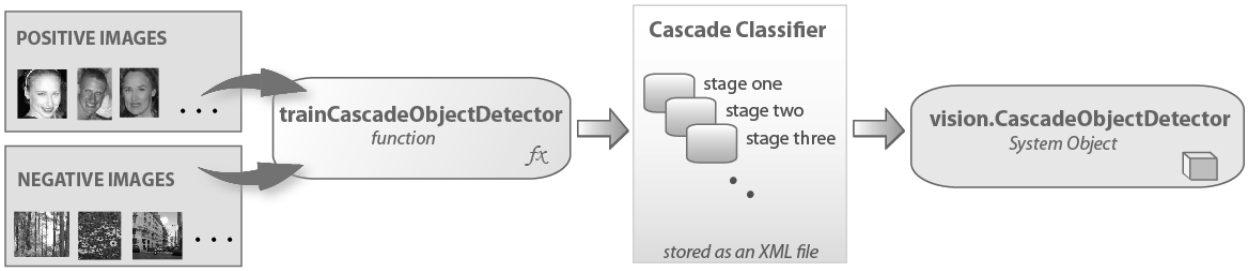

Figure 7.—MATLAB cascade object detector algorithm (Ref. 18).

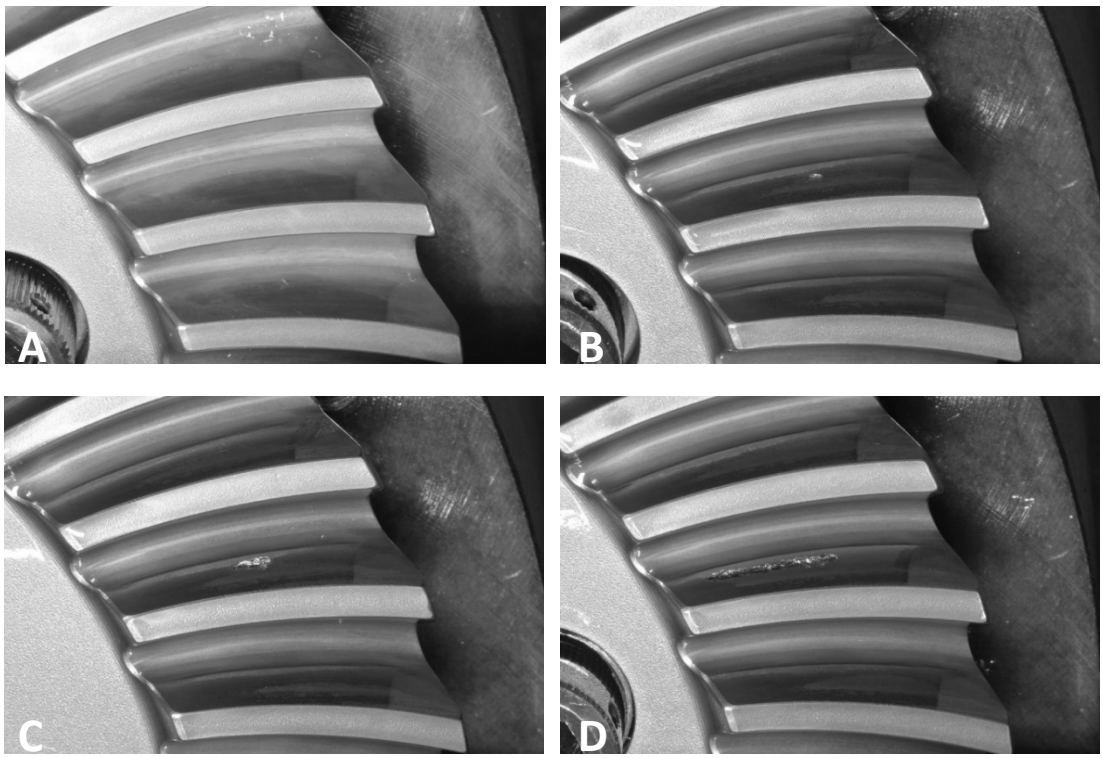

Figure 8.—Control set of gear teeth for pit detector test. Individual center tooth was also used for the control set. (A) no wear, (B) pit, (C) pit, (D) spall.

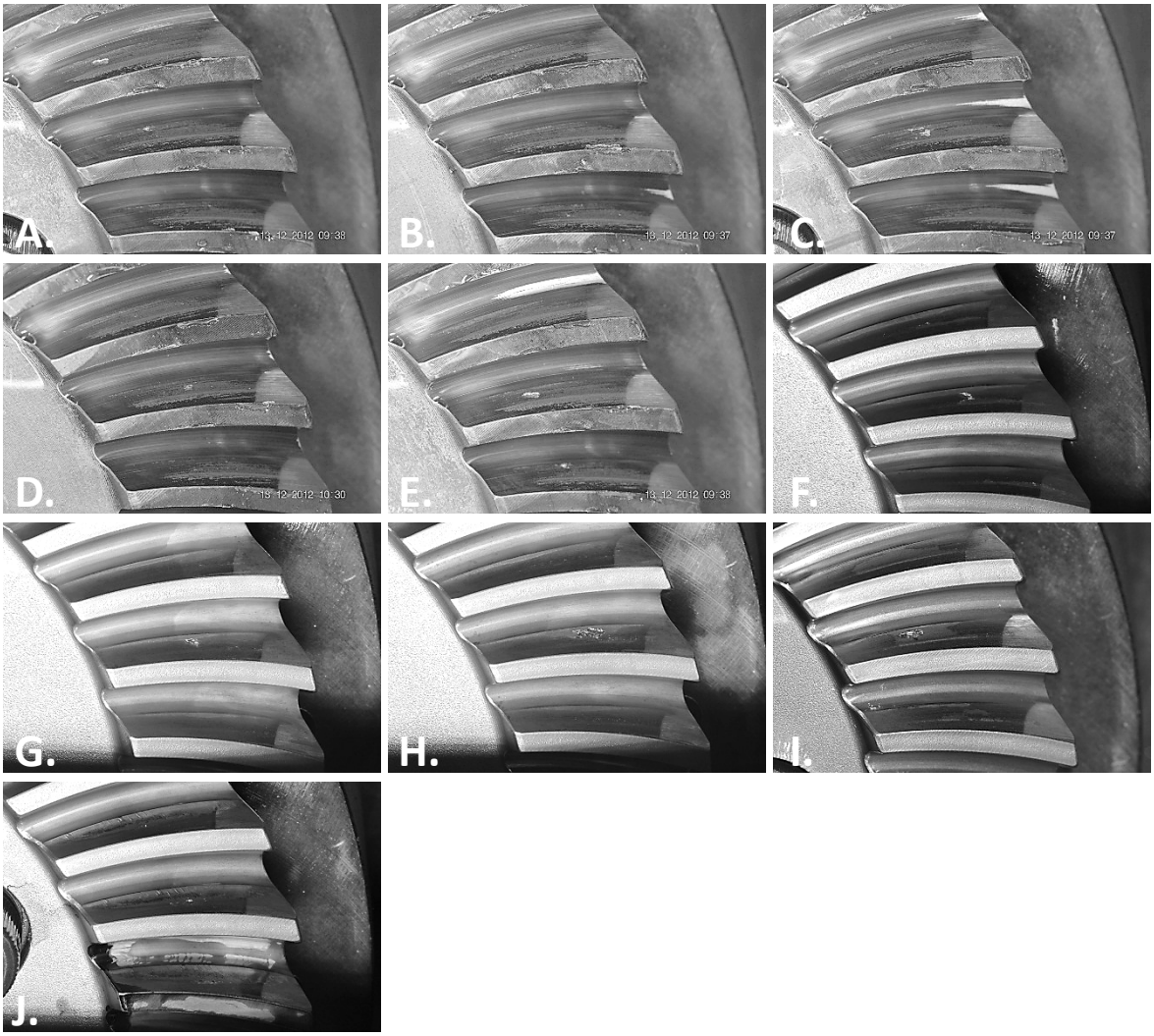

Figure 9.—Gear wear pictures for blind test.

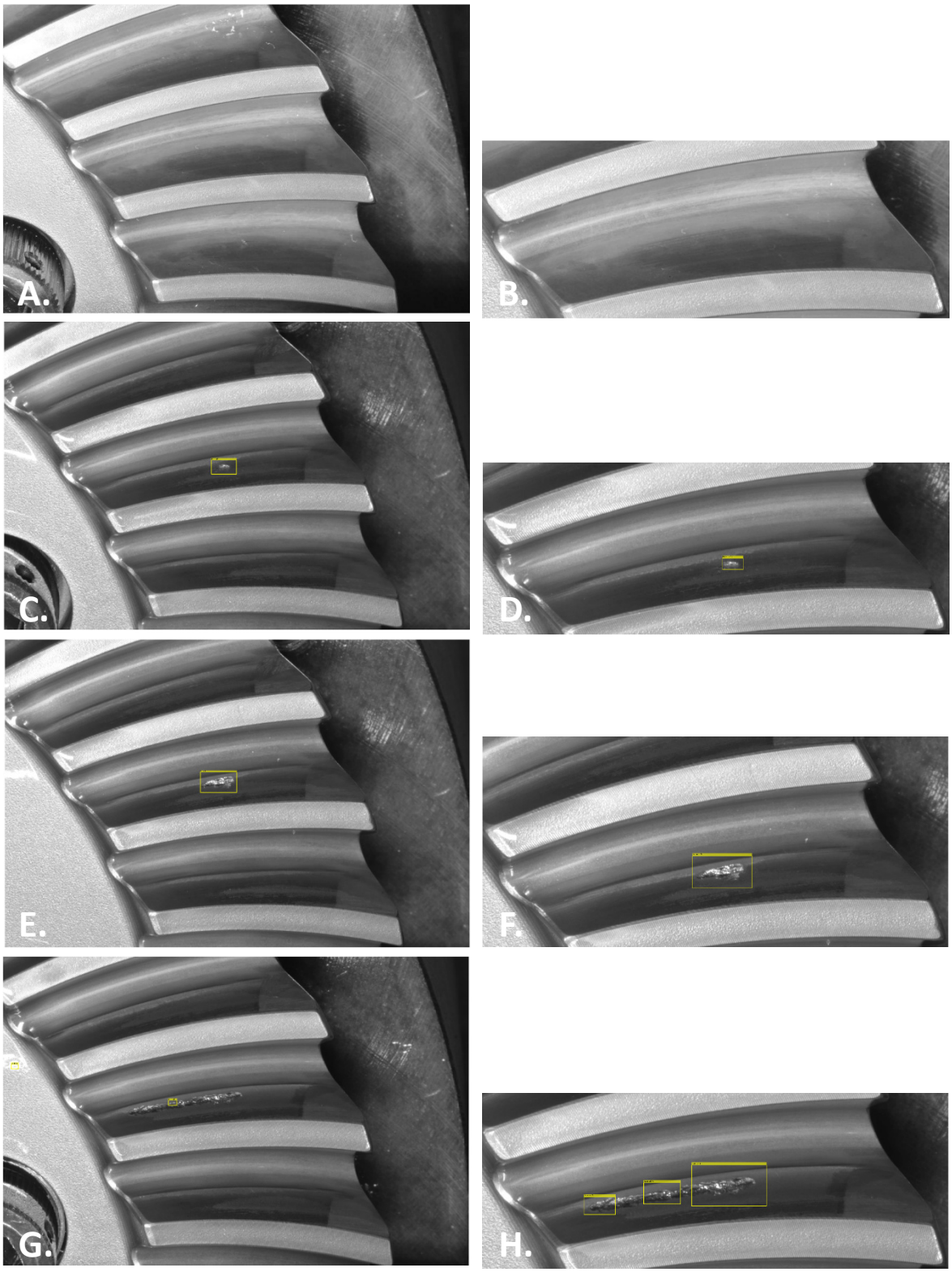

Figure 10.—Results of pit detection algorithm with the control set.

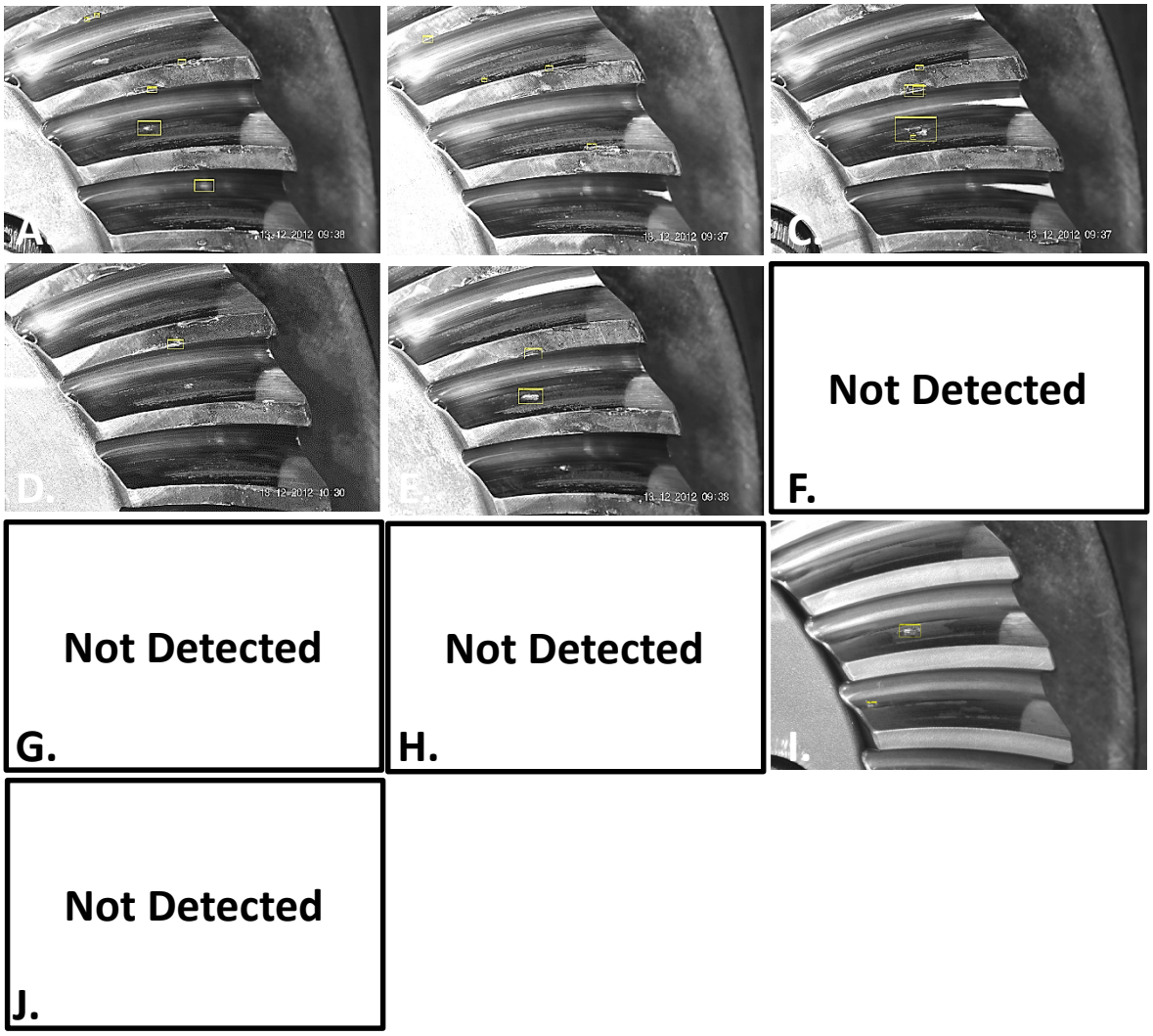

Figure 11.—Results of pit detection algorithm with the blind set.